DAMPING CAPACITY OF A MODEL STEEL STRUCTURE

by

D. Rea[I], R. W. Clough[II], J. G. Bouwkamp[II], and U. Vogel[III]

Synopsis. Dynamic tests have been conducted on a model steel structure consisting of a relatively rigid platform supported by columns. Vibration amplitudes in the dynamic tests barely exceeded yield displacement because fatigue cracks formed in welds at the column bases. Reversed bending tests have also been performed on individual columns of the test structure, and the results of these tests correlate with the dynamic test results. The combined results of both types of test provide a description of the damping capacity of the model structure as a function of amplitude up to the maximum ductility factor obtained.

Introduction. The more energy a structure dissipates while vibrating, the less strength it requires to withstand a prescribed earthquake ground motion. Therefore, the ability to estimate damping capacity of a structure in its design stages should lead to more efficient design for earthquake forces. The damping capacity of a structure vibrating at small amplitudes can be estimated if a dynamic test has been conducted already on a similar type of structure. The results from a number of dynamic tests are available, e.g., (1) and (2)

Even if it were economically feasible to subject a real structure to vibration amplitudes large enough to cause structural damage, existing vibration generators lack sufficient power to do so. In order to determine the damping capacity of real structures vibrating at large amplitudes (in the case of steel structures, amplitudes large enough to cause yielding in a number of members) an alternative approach is required. One approach is to determine experimentally the energy dissipation capacity of individual elements of real structures vibrating at large amplitudes, and then use the results to predict the damping capacity of real structures analytically.

Such an approach seems readily applicable to steel frame structures. Dynamic tests have been conducted on a model steel structure in which the only elements providing lateral stiffness were a pair of identical columns. The vibration amplitudes in the dynamic tests were large enough to cause small amounts of yielding in the columns, and the consequent increase of damping was measured. Reversed bending tests have also been conducted on individual columns and the energy dissipated per cycle in the two types of tests compared. The combined results of both types of tests provide a description of the energy dissipation capacities of a column in its useful range of behavior.

I. Assistant Research Engineer, Department of Civil Engineering, University of California, Berkeley, California, U. S. A.

II. Professor of Civil Engineering, Department of Civil Engineering, University of California, Berkeley, California, U. S. A.

III. Visiting Associate Professor, 1967/68, Department of Civil Engineering, University of California, Berkeley, California, U. S. A.

Model Structure for Dynamic Tests. The model test structure consists of a rectangular platform 10 ft. by 7 ft. in plan, supported by four 5 ft. 5 in. columns, see Fig. 1. The platform is essentially rigid in comparison to the columns and all columns are attached to the platform by pinned connections. Two columns at one end of the platform are attached by pinned connections to plates prestressed to a 2 ft. thick concrete floor slab. The pair of columns at the other end of the platform have their bases prestressed by means of high strength bolts to heavy plates that are also prestressed to the floor slab. The latter pair of columns provide the platform with its resistance to lateral loads in the direction of vibration, and are therefore the columns under test.

Tests have been conducted on a number of types of columns, and the experimental results from two particular types are described below. Both these types of columns, Fig. 1, are fabricated by welding a top plate (6 x 6 x $\frac{1}{2}$ in.) and a base plate (8 x 8 x $1\frac{1}{2}$ in.) to a 5 ft. $2\frac{1}{2}$ in. length of 4 x 4 WF section. In addition, a parabolic strap ($5\frac{1}{2}$ in. long, $\frac{1}{2}$ in. thick) is welded to the base plate and flanges of each column in order to initiate yielding in metal some distance from a weld. One type of column (designated Type 2) differs from the other (Type 1) in having 8 in. long reduced sections in each flange which start $1\frac{1}{2}$ in. above the tops of the parabolic straps. The 4 in. wide flanges are tapered from both ends of the 8 in. section to leave a section 3 in. wide and 5 in. long in the middle, see Fig. 1. The columns are placed in the structure so as to undergo bending about their weak axis.

Dynamic Test Procedures and Experimental Results. Two vibration generators were bolted to the platform of the test structure. These machines (3) were developed at the California Institute of Technology under the supervision of the Earthquake Engineering Research Institute for the Office of Architecture and Construction, State of California. The machines operate on the eccentric-mass principle and consist essentially of two counter-rotating baskets mounted on a common shaft and driven by a $1\frac{1}{2}$ HP DC motor. When weight (the eccentric-mass) is added to the baskets each machine can develop a sinusoidal force. For these tests one machine had sufficient power; the other served only to increase the total mass of the system.

For each value of eccentric mass, the rotational speed of the baskets was increased until the vibration amplitude became significant on approaching resonance. The exciting frequency was then increased in small steps up to resonance and then beyond resonance until the vibration amplitude became insignificant again. Each time the exciting frequency was set at a particular value, the vibration was given sufficient time to become steady-state, and then the response of the structure and the frequency of excitation were recorded.

The response measurements were the displacement and acceleration of the platform and strains at various parts of the columns. Displacement was detected by a $\pm$ 3.0 in. Sanborn differential transformer type displacement transducer, acceleration by a $\pm$ 5 g Statham accelerometer, and strain by SR-4 strain gages of the post-yield type. The signals from the accelerometer and strain gages were recorded by a Honeywell carrier amplifier and ultra-violet recorder (Visicorder) system. The output of

the displacement transducer was fed directly to the Visicorder. Frequency was measured by a digital counter recording the frequency of a signal from a tachometer driven by the DC motor.

Some frequency response curves obtained from the structure with column types 1 and 2 are presented in Fig. 2. The displacement amplitude of the platform is plotted as a function of exciting frequency. The amplitude of the exciting force for each resonance curve is indicated in Fig. 2. (The amplitude of the exciting force increases with the square of the exciting frequency, but since the frequency range covered by the resonance curve is small, changes in the amplitude of the exciting forces are negligible.)

The resonant amplitude of each frequency response curve is plotted against the amplitude of the exciting force for the structure with columns of types 1 and 2 in Fig. 3. Since the resonant amplitude of the structure, $\hat{x}_{res}$, may be related to the exciting force amplitude, $\hat{P}$, by

$$\hat{x}_{res} = \frac{1}{2K\zeta} \hat{P}$$

where K is the spring stiffness and ζ the damping capacity, changes in the slope of these curves may be related to changes in the stiffness of the system, the damping capacity of the system, or changes in both stiffness and damping capacity. The reduction in resonant frequency due to the increase of vibration amplitude for both types of columns is only about 2%, see Fig. 2, so that the stiffness of the system has only decreased by 4% at the largest vibration amplitudes excited. Therefore, the change of slope in a resonant amplitude versus exciting force curve is caused by an increase in damping capacity as the vibration amplitude approaches the yield amplitude.

In the first test, with columns of type 1 in the test structure, the amplitude of the exciting force was increased steadily until the test was terminated by cracks forming in the welds at the base of the columns. However, in the second test with columns of type 2 in the test structure, a smooth curve was obtained only up to the yield amplitude, see Fig. 3. Although the eccentric-mass for frequency response 7 (see Fig. 3) was greater than the eccentric-mass for frequency response 6, the resonant amplitude of frequency response 7 was less than that of 6. The frequency response was observed once more (frequency response 8) and a further reduction in resonant amplitude occurred. The eccentric-mass was then reduced to values below, and then increased to values above, that used in frequency responses 7 and 8, to obtain frequency responses 9 through 19. The latter response curves yielded the middle curve of Fig. 3. After frequency response 19 was observed, the eccentric-mass was again reduced. The above phenomenon was repeated, and the next set of frequency responses, 20 through 28, yielded the lower curve of Fig. 3. In the attempt to obtain a frequency response with a larger resonant amplitude than that associated with frequency response 25, the welds at the base of the column cracked.

Since the resonant frequencies of all the frequency response curves were essentially the same, differences in the curves for column type 2 in Fig. 3 can be attributed to increases in the damping capacity of the

system. Apparently, a number of vibration cycles at amplitudes close to the yield amplitude increases the damping capacity of the structure. (This effect has been reported by Lazan (4) from work in which small specimens were tested in a rotating-bending machine.)

The damping capacity of the model steel frame has been evaluated by two methods. In the first, the bandwidth method, the damping capacity, ζ, is evaluated from

$$\zeta = \frac{\Delta f}{2f_r}$$

where Δf is the difference in frequency of two points on the resonant curve with amplitudes $1/\sqrt{2}$ times the resonant amplitude and f_r is the resonant frequency. The damping capacity evaluated from each resonance curve is indicated in Fig. 2.

In the second method, the damping capacity is evaluated from the ratio of two energy quantities

$$\zeta = \frac{\Delta W}{4\pi W}$$

where ΔW is the energy dissipated per cycle by the structure undergoing steady-state vibration and W is the energy stored in the steady-state vibration.

The energy input per cycle, ΔW, may be evaluated from

$$\Delta W = \pi \hat{P} \hat{x} \sin \varphi$$

where $\hat{P}$ is the amplitude of the exciting force, $\hat{x}$ is the displacement amplitude of the exciting force, and φ is the phase angle by which the response lags the excitation. For these particular tests the values of P and $\hat{x}$ have been evaluated at resonance when $\varphi = 90^{\circ}$ so that $\sin \varphi = 1$.

The energy stored in the steady-state vibration has been assumed equal to the kinetic energy at zero displacement. The effective or generalized mass of the system was evaluated by adding a known weight to the platform and measuring the consequent shift in the resonant frequency. The generalized mass, M, is then calculated from

$$M = -\frac{1}{2}\frac{\Delta M}{\Delta \omega}\ \omega_r$$

where ΔM is the mass of the added weight, ω_r is the resonant frequency of the system, and $\Delta\omega$ is the change in resonant frequency caused by the addition of ΔM. By this means the generalized mass of the structure was found to be 3540/g lb. The kinetic energy at zero displacement is given by

$$W = \tfrac{1}{2} M\hat{v}^2 = \tfrac{1}{2} M\omega^2 \hat{x}^2$$

where $\hat{v}$ is the velocity of the generalized mass at zero displacement.

The damping capacity of the test structure with columns of type 1 and 2 is shown as a function of resonant amplitude in Fig. 4. For each resonant amplitude the damping capacity has been evaluated by both the bandwidth and energy-ratio methods, and in every case the results agreed. The results of both methods are plotted for column type 1, but only the results from the energy-method are plotted for column type 2.

The dynamic tests showed that the damping capacity increased sharply once the vibration amplitude approached the yield displacement of the columns. Due to the large number of cycles that are accumulated by the method of testing, it was only possible to initiate yielding in column type 1 before fatigue cracks developed in the welds at the base of the columns. However, even the vibration amplitudes achieved have been sufficient to increase the damping capacity from 0.16% in the so-called elastic range to 1.06% in the case of the test structure with columns of type 1, and from 0.15% to 1.2% for the structure with columns of type 2.

Reversed Loading Tests. The damping capacity of an individual column can be obtained by subjecting it to slowly reversing loads similar to those described by Popov (5). Since the number of cycles accumulated in such a test is small, the problem of fatigue is circumvented, and thus the columns can be subjected to displacement cycles of larger amplitudes than the maximum amplitudes achieved in the dynamic tests described above. Reversed loading tests were performed on columns of both types 1 and 2 in order to establish some correlation between the results from the reversed bending tests and from the dynamic tests.

The rig employed to subject the columns for reversed loading tests is the one previously described by Bertero and Popov (6). When a specimen is installed in the rig (in this case a column of either type 1 or 2) it acts as a cantilever. Vertical alternating loads may then be applied to the free end of the cantilever by means of a hydraulic jack. The force applied to the specimen is measured by a load-cell interposed between the jack's piston and the free end of the cantilever. The force transmitted by the load cell, the displacement of the free end of the cantilever, and strains at various locations in the specimen were recorded by the same system used in the dynamic tests.

In testing a specimen, the load applied to the free end of the cantilever was cycled two or three times at constant displacement amplitude until a stable hysteresis loop was established. The force, displacement, and strains were recorded over the next two cycles. The constant displacement amplitude was then increased and the process repeated. Initially the constant amplitudes were smaller than the yield displacement of the specimen, and they were increased in a number of steps up to a ductility factor between 3 and 4. The force applied to the beam was plotted against displacement over each cycle to obtain hysteresis loops for the specimen. Some hysteresis loops obtained for a column of type 1 are shown in Fig. 5.

The energy dissipated per cycle by the structure equals the area within the hysteresis loop, which was measured by means of a planimeter. Twice the energy dissipated per cycle by a column of type 1 and 2 is plotted as a function of the displacement amplitude of the cycle in Fig. 6. The energy dissipated per cycle by the test structure (measured in the

dynamic tests) is also included in Fig. 6. Over the displacement amplitude range common to both methods of testing, the methods agree on the quantity of energy dissipated per cycle.

The hysteresis loops for the columns represent the force-deformation relationships of the structure, assuming rate of loading effects are negligible. On this assumption, the damping capacity of the structure may be evaluated from the hysteresis loops of the columns. To evaluate the damping capacity the energy ratio method may be used where ΔW is the energy represented by the area within the hysteresis loop, and W is a quantity of energy associated with the hysteresis loops that makes ζ dimensionless. However, there are four basic ways that W may be defined which lead to four definitions of ζ. The four ways to define W are illustrated by means of a Ramberg-Osgood type force-deformation relationship shown in Fig. 7. They are: $W_1 = A+B+C+D+E$, $W_2 = D+E$, $W_3 = C+D+E$, and $W_4 = E$, where the letters A through E designate the areas of spaces in which the letters are immediately enclosed by either solid or dashed lines. If the definition of damping corresponding to W_1, W_2, W_3, and W_4 are ζ_1, ζ_2, ζ_3, and ζ_4, then the definition of damping capacity ζ_1, has been used by Hudson (7), the definition ζ_2 by Rosenblueth and Herrera (8), as well as Berg (9), and definition ζ_3 by Jacobsen (10) and Hudson (7). These definitions of damping capacity have been discussed by Jennings (11).

The damping capacities implicit in the hysteresis loops of a column of type 1 (Fig. 5) have been evaluated according to definitions ζ_1, ζ_2, ζ_3, and ζ_4. (For each hysteresis loop, the areas ΔW, W_3 and W_4 were measured by planimeter and the areas W_1 and W_2 calculated.) The damping capacities determined from the dynamic tests and reversed bending tests are compared on a semi-log scale in Fig. 8. The curve obtained from the dynamic tests is continuous with the curves obtained from the reversed bending tests.

The damping capacity evaluated from the hysteresis loops is plotted as a function of ductility factor (ratio of amplitude to yield amplitude) in Fig. 9. The damping capacity evaluated from definition ζ_1 is plotted over the complete range for which it was determined: 0.8 to 3.8. The damping capacity evaluated from the definitions ζ_2, ζ_3 and ζ_4 are plotted only in the range of ductility factor 1.3 to 3.8 since below a ductility factor of 1.3 all four definitions agree. The damping capacities obtained from the dynamic tests are also included in Fig. 9 so that the damping capacity of the test structure is completely described up to a ductility factor of 3.8, assuming rate of loading effects are negligible (which seems to be true from the results of these particular tests).

At amplitudes of vibration below $0.8X_y$ the damping capacity of the model structure with columns of type 1 is essentially independent of amplitude with magnitude 0.15%. At amplitudes above $0.8X_y$ the damping capacity increases with vibration amplitude (an effect observed by Lazan (4) from tests conducted on small specimens) attaining a value of 3.0% at a ductility factor of 1.53, the ductility factor at which a full plastic hinge forms for a column of type 1. As displacement amplitude increases above a ductility factor of 1.53, the damping capacity continues to increase but at a rate which depends on the definition of damping

dynamic tests) is also included in Fig. 6. Over the displacement amplitude range common to both methods of testing, the methods agree on the quantity of energy dissipated per cycle.

The hysteresis loops for the columns represent the force-deformation relationships of the structure, assuming rate of loading effects are negligible. On this assumption, the damping capacity of the structure may be evaluated from the hysteresis loops of the columns. To evaluate the damping capacity the energy ratio method may be used where ΔW is the energy represented by the area within the hysteresis loop, and W is a quantity of energy associated with the hysteresis loops that makes ζ dimensionless. However, there are four basic ways that W may be defined which lead to four definitions of ζ. The four ways to define W are illustrated by means of a Ramberg-Osgood type force-deformation relationship shown in Fig. 7. They are: $W_1 = A+B+C+D+E$, $W_2 = D+E$, $W_3 = C+D+E$, and $W_4 = E$, where the letters A through E designate the areas of spaces in which the letters are immediately enclosed by either solid or dashed lines. If the definition of damping corresponding to W_1, W_2, W_3, and W_4 are ζ_1, ζ_2, ζ_3, and ζ_4, then the definition of damping capacity ζ_1, has been used by Hudson (7), the definition ζ_2 by Rosenblueth and Herrera (8), as well as Berg (9), and definition ζ_3 by Jacobsen (10) and Hudson (7). These definitions of damping capacity have been discussed by Jennings (11).

The damping capacities implicit in the hysteresis loops of a column of type 1 (Fig. 5) have been evaluated according to definitions ζ_1, ζ_2, ζ_3, and ζ_4. (For each hysteresis loop, the areas ΔW, W_3 and W_4 were measured by planimeter and the areas W_1 and W_2 calculated.) The damping capacities determined from the dynamic tests and reversed bending tests are compared on a semi-log scale in Fig. 8. The curve obtained from the dynamic tests is continuous with the curves obtained from the reversed bending tests.

The damping capacity evaluated from the hysteresis loops is plotted as a function of ductility factor (ratio of amplitude to yield amplitude) in Fig. 9. The damping capacity evaluated from definition ζ_1 is plotted over the complete range for which it was determined: 0.8 to 3.8. The damping capacity evaluated from the definitions ζ_2, ζ_3 and ζ_4 are plotted only in the range of ductility factor 1.3 to 3.8 since below a ductility factor of 1.3 all four definitions agree. The damping capacities obtained from the dynamic tests are also included in Fig. 9 so that the damping capacity of the test structure is completely described up to a ductility factor of 3.8, assuming rate of loading effects are negligible (which seems to be true from the results of these particular tests).

At amplitudes of vibration below $0.8X_y$ the damping capacity of the model structure with columns of type 1, is essentially independent of amplitude with magnitude 0.15%. At amplitudes above $0.8X_y$ the damping capacity increases with vibration amplitude (an effect observed by Lazan (4) from tests conducted on small specimens) attaining a value of 3.0% at a ductility factor of 1.53, the ductility factor at which a full plastic hinge forms for a column of type 1. As displacement amplitude increases above a ductility factor of 1.53, the damping capacity continues to increase but at a rate which depends on the definition of damping

Acknowledgement

The work described above was sponsored partly by the American Iron and Steel Institute under AISI Project No. 140 and partly by the National Science Foundation under Grant NSF GK-1319. The authors wish to express their appreciation to both sponsors.

References

1. Nielsen, N. N., "Vibration tests of a Nine-Story Steel Frame Building," Proc. ASCE, J. Engineering Mechanics Division, Vol. 92, No. EM 1, 1966.

2. Rea, D., J. G. Bouwkamp and R. W. Clough, "The Dynamic Behavior of Steel Frame and Truss Buildings," Structures and Materials Research Report No. 66-24, University of California, Berkeley, California, 1966.

3. Hudson, D. E., "Resonance Testing of Full-Scale Structures," Proc. ASCE, J. Engineering Mechanics Division, Vol. 90, No. EM 3, 1964.

4. Lazan, B. J., "Energy Dissipation Mechanisms in Structures, With Particular Reference to Material Damping," Structural Damping (Editor: J. E. Ruzicka), ASME, 1959.

5. Popov, E. P., "Reliability of Steel Beam to Column Connections Under Cyclic Loading," Proc. Fourth World Conference on Earthquake Engineering, Chile, 1969.

6. Bertero, V. V., and E. P. Popov, Effect of Large Alternating Strains of Steel Beams," Proc. ASCE, J. Structural Division, Vol. 91, St. 1, 1965.

7. Hudson, D. E., "Equivalent Viscous Friction for Hysteretic Systems With Earthquake-like Excitations," Proc., Third World Conference on Earthquake Engineering, New Zealand, 1965.

8. Rosenblueth, E., and I. Herrera, "On a Kind of Hysteretic Damping," Proc. ASCE, J. Engineering Mechanics Division, Vol. 90, No. EM 4, 1964.

9. Berg, G. V., "A Study of the Earthquake Response of Inelastic Systems," Preliminary Reports presented at the 1965 annual meeting of the Structural Engineers' Association of California, AISI.

10. Jacobsen, L. S., "Damping in Composite Structures," Proc., Second World Conference on Earthquake Engineering, Japan, 1960.

11. Jennings, P. C., "Equivalent Viscous Damping for Yielding Structures," Proc. ASCE, J. Engineering Mechanics Division, Vol. 94, No. EM 1, 1968.

12. Jennings, P. C., "Periodic Response of a General Yielding Structure," Proc. ASCE, J. Engineering Mechanics Division, Vol. 90, No. EM 2, 1964.

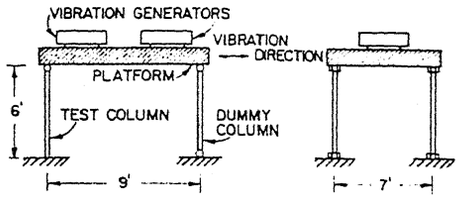

(a) ELEVATION AND END ELEVATION: TEST STRUCTURE

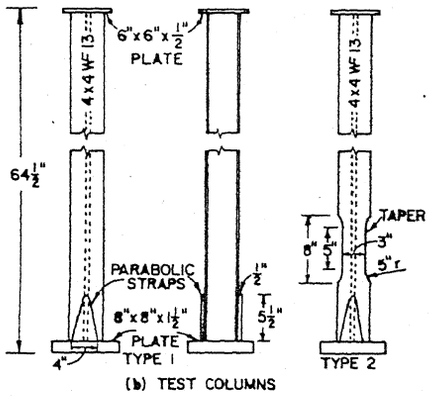

(b) TEST COLUMNS

FIG. 1 DETAILS OF TEST STRUCTURE AND COLUMNS

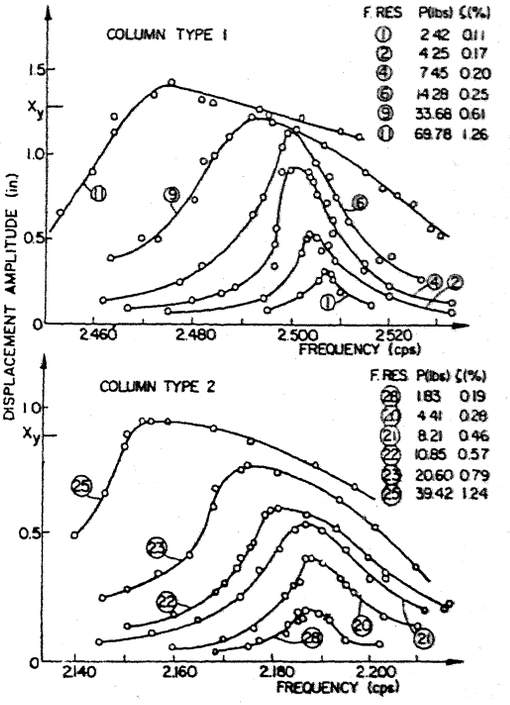

FIG. 2 FREQUENCY RESPONSES OF STRUCTURE

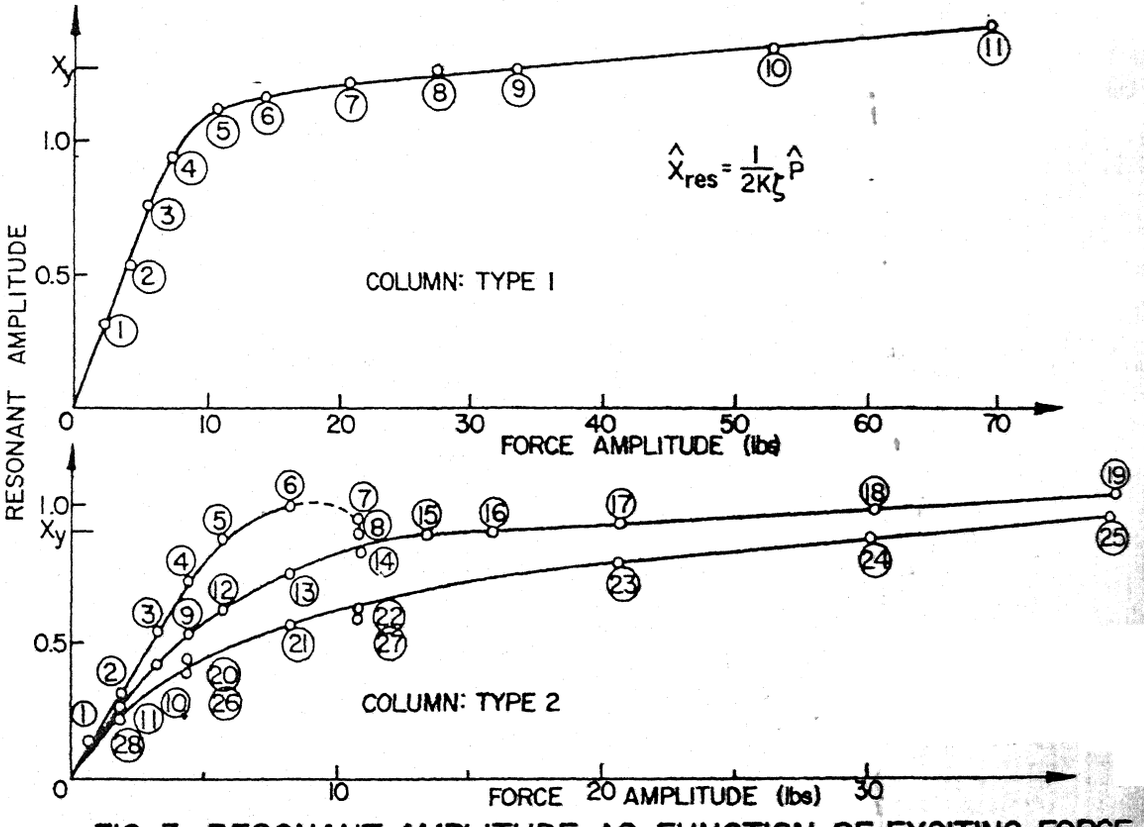

FIG. 3 RESONANT AMPLITUDE AS FUNCTION OF EXCITING FORCE

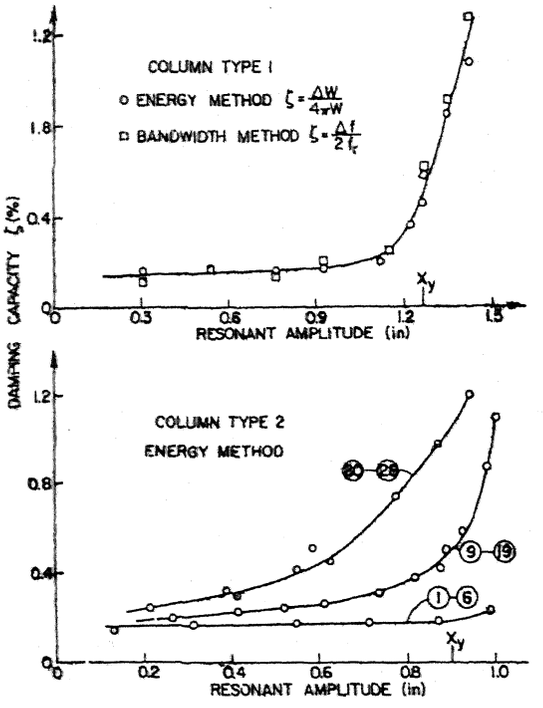

FIG. 4 DAMPING CAPACITY OF STRUCTURE

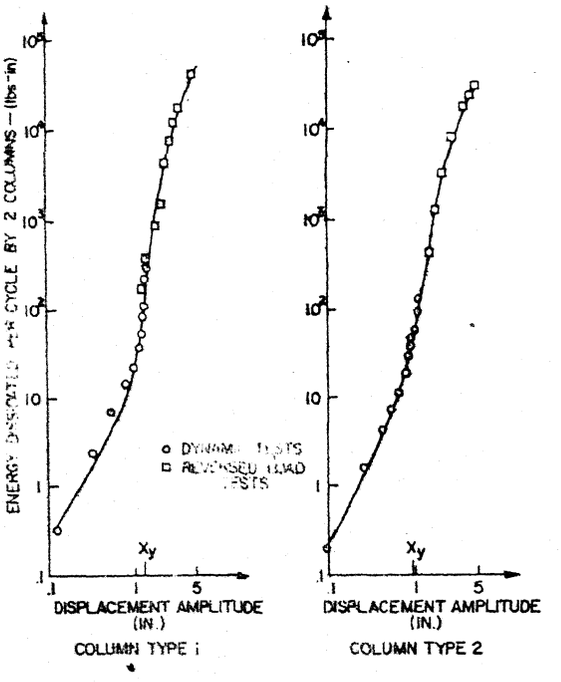

FIG. 6 ENERGY DISSIPATED IN REVERSED LOAD TESTS AND DYNAMIC TESTS

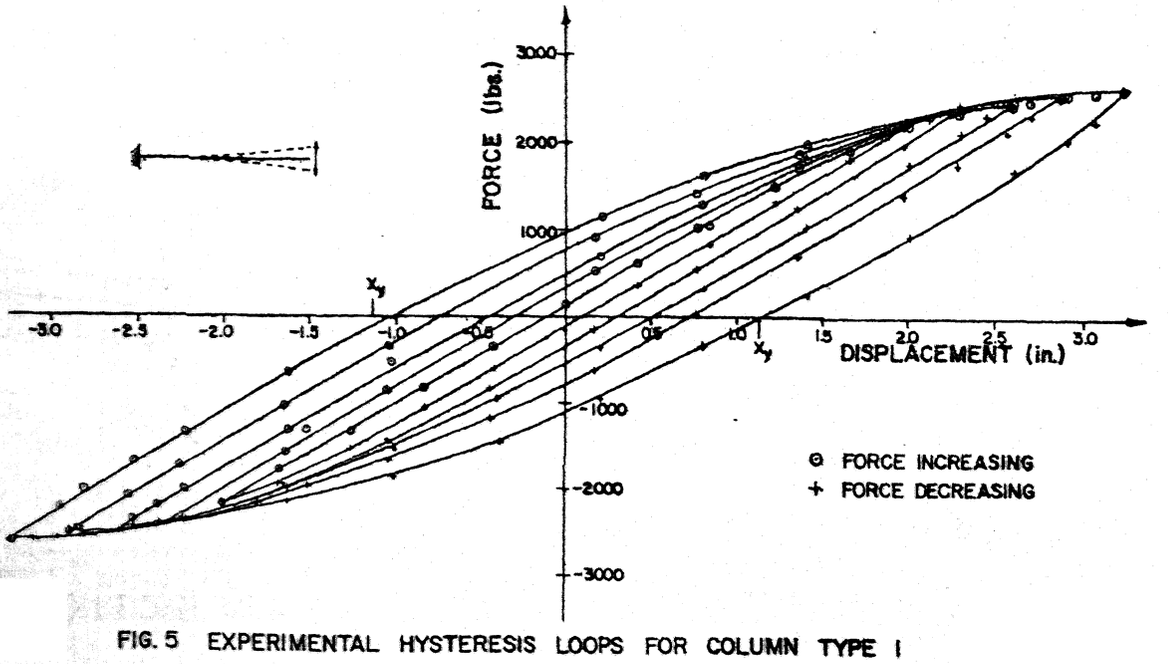

FIG. 5 EXPERIMENTAL HYSTERESIS LOOPS FOR COLUMN TYPE I

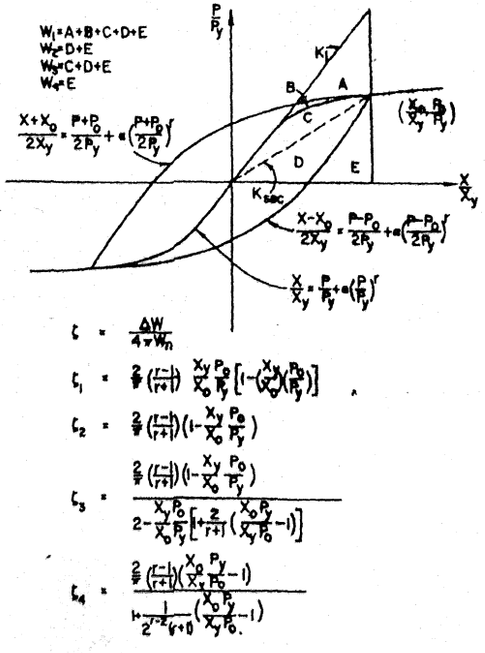

FIG. 7 RAMBERG-OSGOOD TYPE FORCE-DEFORMATION RELATIONSHIP AND DIFFERENT DAMPING VALUES

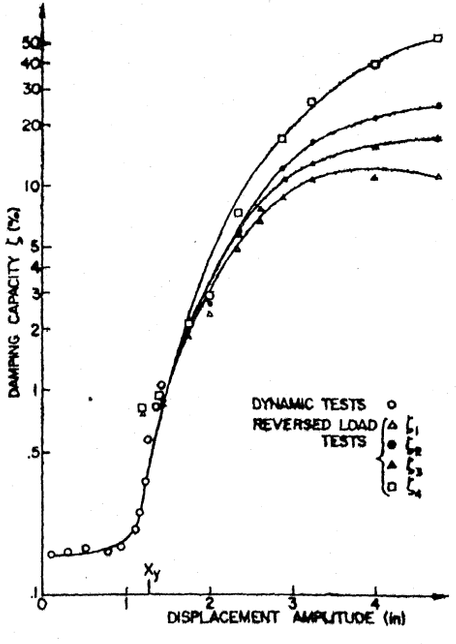

FIG. 8 DAMPING CAPACITY FOR COLUMN TYPE I

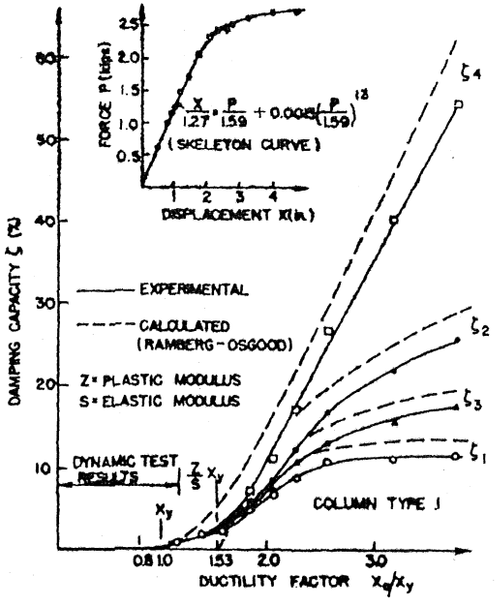

FIG. 9 COMPARISON OF CALCULATED (RAMBERG-OSGOOD) AND EXPERIMENTAL DAMPING CAPACITIES